

Airborne and Ground IP: an integrated approach for exploration

F. Dauti¹, A. Viezzoli², G. Fiandaca¹

¹ *The EEM Team for Hydro & eXploration, Dep. of Earth Sciences A. Desio, Università degli Studi di Milano, Via Botticelli 23, Milano (Italy)*

² *Emergo s.r.l., Via XX Settembre 12, Cascina (Pisa), Italy*

General Introduction

The Iberian Pyrite Belt (IPB) is one of the oldest and still active mining districts in the world. In the last decade, a renewed mining activity and scientific research have led into a wealth of new data and new geological hints for explorers and for the academic community, making the IPB one of the most important and dynamic mining districts in Europe (Inverno et al, 2015). In this region, the great number of different signatures related to the ore body and to its vectors call for an integrated use of complementary geophysical methods. The sulfides targets show contrast in both density and electrical properties, and historically gravity has played a crucial role for exploring in the IPB. These methods have been later accompanied by EM methodologies, both airborne and ground, given their high sensitivity to conductive targets (Menghini et al, 2022).

With this contribution we will focus on an application of a novel modelling approach that aims to properly extract the Induced Polarization (AIP) effects from the Airborne Electromagnetic (AEM) data. The AEM survey has been acquired in the IPB for mineral exploration to localize the VMS deposit. After the AIP modelling, we will show a comparison between the airborne chargeability and some overlapping ground IP models from the same area. This comparison aims to better understand the potential in the use of AIP for exploration and to attempt an improvement in the definition of the sensitivity field of the airborne technique, as well as its relationships with ground IP. Then, a joint inversion between the two methods will be presented.

Inductive Induced Polarization - theory and modelling

It is known and accepted that the Electromagnetic methods are sensitive to Induced Polarization effects (AIP) when acquired over a polarizable medium (Kratzer and Macnae, 2012; Viezzoli et al., 2013). From a physical point of view, the polarization processes generate currents in the ground (polarization currents) with an opposite direction respect to the pure EM currents (eddy currents) that proceed downward with a diffusive regime. These effects generate a distortion of the recorded electromagnetic signal which often culminate in its change of sign at late times when the halfspace is

particularly polarizable. In general, the distortions generated from IP have two signatures in the EM data: a faster decay (respect to the purely resistive forward response) and/or negative voltages. Under these conditions, the standard EM modelling, which does not account for polarization currents, ceases to be valid (Smith and Klein, 1996): the negative data cannot be fitted and the fast-decaying signals are modelled as strong resistors, generating artifacts.

To avoid the mis-modelling of EM-IP affected data, it is necessary to use a dispersive-resistivity model (such as the Cole & Cole one) to compute the forward response and considering the capacitive nature of the ground. This approach gives the opportunity to map, as well as the resistivity, the chargeability of the ground that is often related to significant economic (or signatures of) mineralization. At the same time, it complicates the inversion process adding three more parameters and expanding the model space generating equivalent domains. It follows that an appropriate parameters management during the inversion process is crucial to properly retrieve the ground description and to maximize the AIP sensitivity to geological and mineral targets.

Geophysical and geological description

The Airborne EM data have been acquired in spring 2022 with the NRG XCite Time Domain system, with a 25Hz base frequency, and the acquisition lines are illustrated in black lines in *figure 1*. In the same area, 18 SyscalPro lines (0.125Hz of base frequency, 50% duty cycle) of ground Time Domain DCIP have been acquired (red lines in *figure 1*).



Figure 1. Survey location. In black the Airborne EM lines are displayed, in red the DCIP.

In the base map of *figure 1* the local geology is shown. Two main domains are visible: a volcanic intrusive one in the north, where Rhyolite and Dacite are presented in red and green, and a more recent sedimentary domain that covers the outcrop is in yellow in the southern area. The main tectonic features are represented in black and outcrops in the northernmost part of the investigated area.

Data modelling and inversion

Among the differences between Airborne and Ground IP, the most obvious are in the footprint, depth of investigation and spectral content, with AEM data's frequency bandwidth usually a couple of orders of magnitudes higher than that of ground IP data. Beside these problems, another major issue, not always recognized, is the difference in the modelling approach. Ground IP data is usually modelled dropping the spectral information, e.g., turning a full secondary voltage decay into a single value of integral chargeability (e.g. Oldenburg and Li, 1994). Moreover, the effect of current waveform is often not modelled, resulting in inversion models in which the retrieved polarization magnitude strongly depends on the acquisition settings of the current waveform, making a quantitative comparison between AIP and Ground IP impossible (Olsson et al., 2019).

On the contrary, in this study we model the IP spectral content in both AIP and Ground IP data with the same modelling approach, in terms of data-preparation, model space management and inversion approach.

In particular, the galvanic data have been modelled in 2D in terms of full-voltage decay (instead of the integral chargeability), taking into account the transmitter waveform and the receiver transfer function (Fiandaca et al., 2012; Fiandaca et al., 2013; Bollino and Fiandaca, 2024). The inductive data have been modelled in 1D, and to reduce the model space and to enhance the spectral resolution, the frequency dependence and time constant parameters have been set to vary only horizontally (while resistivity and maximum phase change also with depth).

For both the methos, the Maximum Phase Angle (MPA) re-parametrization of the Cole & Cole model has been used (Fiandaca et al., 2018). In the MPA Cole-Cole model, the maximum phase φ_{max} of the complex conductivity and the phase relaxation time τ_φ are used instead of m_0 and τ_ρ (of the classic Cole & Cole model). The phase of the complex conductivity can be defined in terms of both *equations 1 and 2* as:

$$\varphi(\omega) = tg^{-1} \left(\frac{\sigma''(\omega)}{\sigma'(\omega)} \right) = -tg^{-1} \left(\frac{\rho''(\omega)}{\rho'(\omega)} \right) \quad (\text{eq.1})$$

The phase reaches his maximum φ_{max} at an angular frequency $\omega \equiv 1/\tau_\varphi$ as:

$$\varphi_{max} = tg^{-1} \left(\frac{\sigma''(1/\tau_\varphi)}{\sigma'(1/\tau_\varphi)} \right) = tg^{-1} \left(\frac{\rho''(1/\tau_\varphi)}{\rho'(1/\tau_\varphi)} \right) \quad (\text{eq. 2})$$

Finally, the model space of the MPA Cole-Cole model can be written as:

$$m_{MPA\ Cole-Cole} = \{\rho_0, \varphi_{max}, \tau_\varphi, C\}$$

The MPA parametrisation replace the strongly-correlated parameters m_0 and C of the classic Cole-Cole model with the weakly-correlated parameters φ_{max} and C (Fiandaca et al., 2018), to improve the resolution retrieved from inversion IP data of the classical Cole-Cole model.

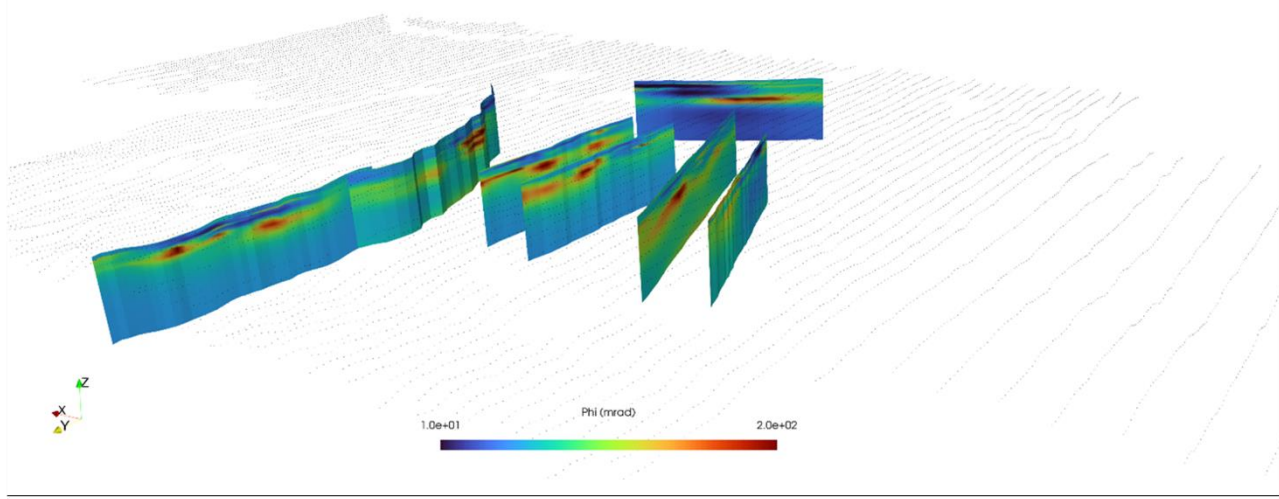
The inversions have been performed with the inversion with EEMverter (Fiandaca et al., 2024), following a modelling scheme that uses voxel model mesh to map the solved parameters via an interpolation of the forward mesh solutions. The decoupling of the model mesh and the forward mesh allows to work with more flexible and manageable

spaces (forward and model) to perform joint inversions and time laps inversions. In our inversion procedure, in order to increase the parametrical resolution and the phase sensitivity in depth, we parametrized the spectral parameters (τ_ϕ , C) on an independent mesh respect to resistivity and phase, with different lateral constraints and vertically fixed (as proposed by Viezzoli and Fiandaca in 2021).

Results

In *figure 2a* and *2b* the results are shown, with a comparison between a portion of the airborne and the ground DCIP modelled chargeability (phase) with our modelling approach.

a)



b)

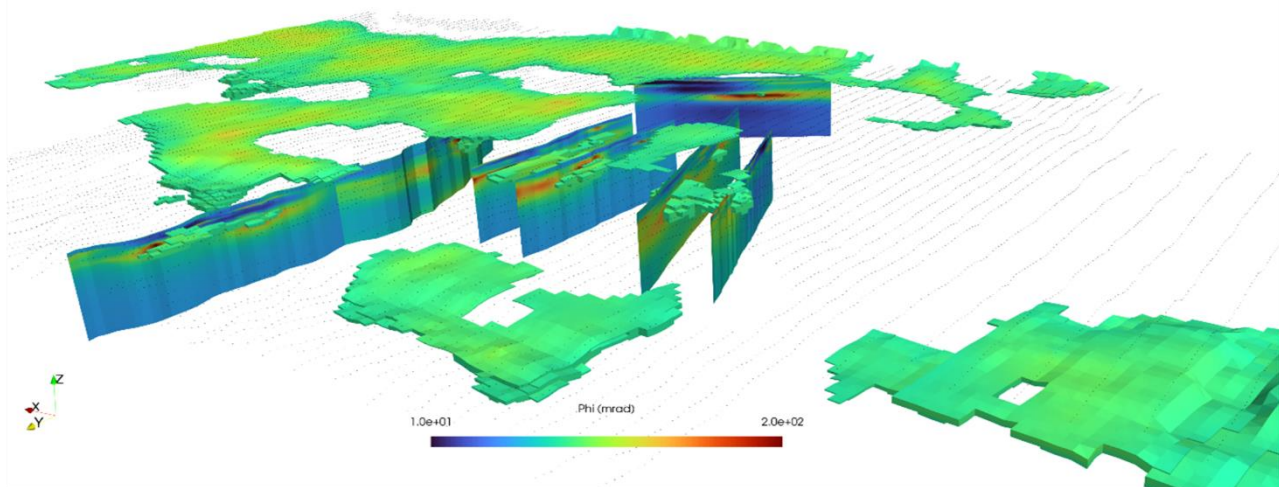


Figure 2. a) Example of ground DCIP phase results and, in dashed line, the AEM survey flown above; b) Partial Ground DCIP vs Airborne IP phase results

As visible from the figures, a great correlation between the airborne and ground is obtained when modelling with the presented approach. The airborne chargeability model shows a consistent structure with the ground model in depth and a geology-controlled behaviour in the shallower near surface. A known mineralization has also been mapped with the AIP. The differences in the near surface are consequence of the big electric dipoles dimension used for the ground DCIP (100m). For this dataset, all the airborne IP chargeability anomalies have been confirmed from the ground IP.

After this, we performed a joint inversion between all the ground DCIP lines (17) and the entire AEM survey. For the joint inversion we used the AEM model (for all the parameters) as starting model for the joint inversion. In *figure 3* the results are shown.

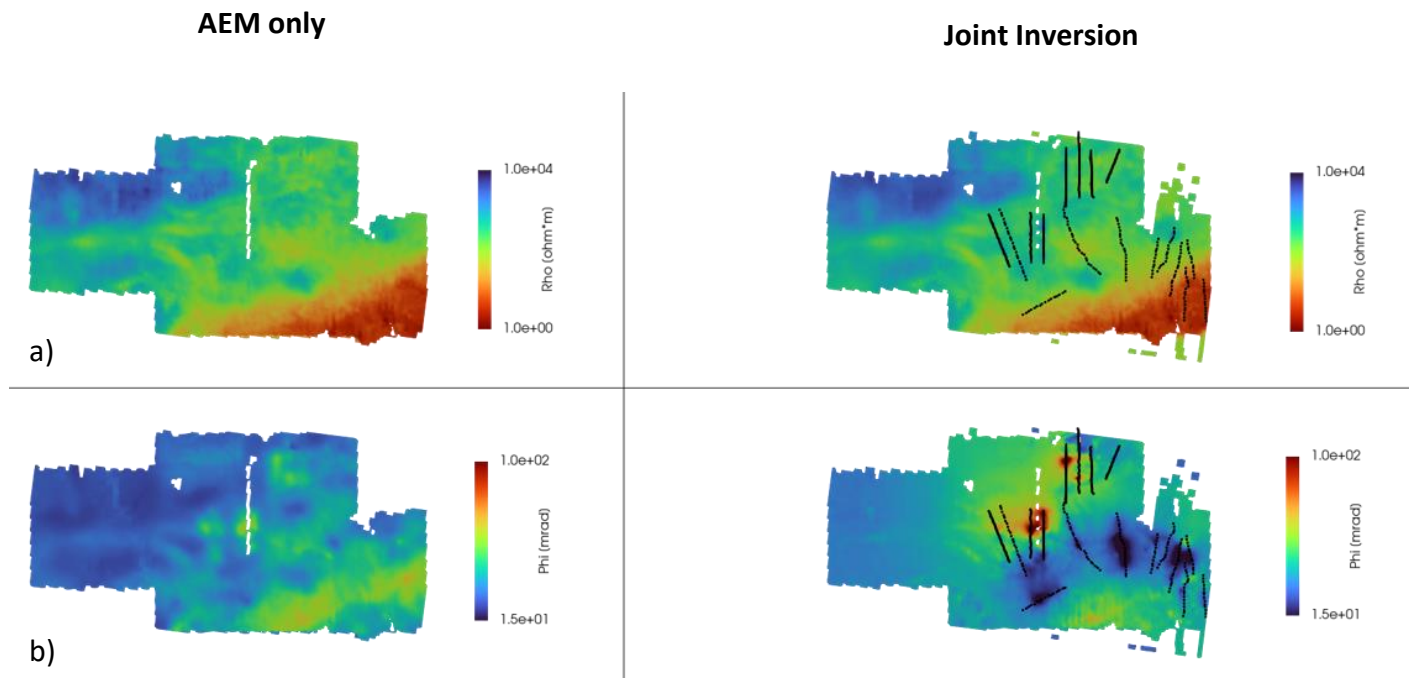


Figure 3. Comparison between AEM only model (on the left) and Joint Inversion model (on the right) for a slice at 60 m of depth. Figure 3a shows a comparison between the resistivities while figure 3b a comparison between chargeabilities.

In *figure 3a* a comparison between the AEM only and joint inversion resistivity is presented. As visible, the main structural are mantained in the inversions. Differently, in *figure 3b*, it appears that introducing the ground DCIP lines in the inversion add structure in the chargeability model for the entire survey area. In terms of misfit, the general misfit of the AEM only inversion is 1.6 while the misfit for the joint inversion is 1.7, confirming how the AEM data accept the jointly obtained chargeability model obtained together with the ground IP.

Conclusions

This study shows encouraging results in the using of the Airborne Induced Polarization for chargeability mapping for airborne-scale areas. In particular it results that:

- Reducing the equivalences in the AEM-IP modelling is a key to unlock the understanding of the AIP sensitivity to geological and mineral targets.
- For this case study, the airborne chargeability shown sensitivity to deep chargeable bodies.
- All of the airborne chargeability anomalies have been confirmed from the ground DCIP models, demonstrating an overlapping field of sensitivity between the methods.
- Known mineralizations have been mapped with the AIP.
- The joint inversion between the DCIP and the AIP is possible and shows how the AEM data not only is compatible with the joint model, but also contribute in the chargeability mapping.

References

Bollino, A., Fiandaca G. (2024). Full-decay spectral modelling of time-domain induced polarization decoupling model and forward meshes. GNGTS 2024, 13-16 February 2024, Ferrara, Italy.

Fiandaca, G., Gazoty, A., Auken, E., & Christiansen, A. V. (2012). Time-domain-induced polarization: Full-decay forward modeling and 1D laterally constrained inversion of Cole-Cole parameters. *Geophysics*, 77, E213-E225.

Fiandaca, G., Ramm, J., Binley, J., Gazoty, A., Christiansen., A.V., Auken, E., Resolving spectral information from time domain induced polarization data through 2-D inversion, *Geophysical Journal International*, Volume 192, Issue 2, February 2013, Pages 631–646.

Fiandaca, G., Madsen, L.M. and Maurya, P.K. (2018), Re-parameterisations of the Cole-Cole model for improved spectral inversion of induced polarization data. *Near Surface Geophysics*, 16: 385-399.

Fiandaca, G., Zhang, B., Chen, J., Signora, A., Dauti, F., Galli, S., Sullivan, N.A.L., Bollino, A., Viezzoli, A. (2024). EEMverter, a new 1D/2D/3D inversion tool for Electric and Electromagnetic data with focus on Induced Polarization. GNGTS 2024, 13-16 February 2024, Ferrara, Italy.

Inverno, C. & Díez-Montes, A. & Rosa, Carlos & Garcia-Crespo, Jesus & Matos, João & García-Lobón, J. & Carvalho, João & Bellido, F. & Castello-Branco, J. & Ayala, Conxi & Batista, M. & Rubio, Felix Manuel & Granado, Isabel & Tornos, F. & Oliveira, Jose & Rey, C. & Araujo, Vitor & Sanchez-Garcia, Teresa & Pereira, Zelia & Sousa, P., (2015). Introduction and Geological Setting of the Iberian Pyrite Belt. 10.1007/978-3-319-17428-0_9.

Kratzer, T. and Macnae, J., 2012, Induced polarization in airborne EM, *Geophysics*, 77(5), E317–E327.

Oldenburg, D.W. & Li, Y., 1994. Inversion of induced polarization data, *Geophysics*, 59, 1327–1341.

Leistel, J.M., Marcoux, E., Thieblemont., D., Quesada, C., Sanchez, A., Almodovar G.R., Pascual, E., Saez, R., (1998). The volcanic-hosted massive sulphide deposits of the Iberian Pyrite Belt. Review and preface to the special issue: *Mineralium Deposita*, v. 33, p. 2-30

Menghini, A., Fernandez, I., Viezzoli, A., Pushing Exploration in the Pyrite Belt Around Aem, Conference Paper, NSG2022 3rd Conference on Airborne, Drone and Robotic Geophysics, Sep 2022, Volume 2022, p.1 – 5, Belgrade, Serbia.

Olsson, P. I., Fiandaca, G., Maurya, P. K., Dahlin, T., & Auken, E. (2019). Effect of current pulse duration in recovering quantitative induced polarization models from time-domain full-response and integral chargeability data. *Geophysical Journal International*, 218(3), 1739-1747.

Pelton W.H., Ward S.H., Hallof P.G., Sill W.R., Nelson P.H. Mineral discrimination and removal of inductive coupling with multifrequency IP, *Geophysics*, 1978, vol. 43 (pg. 588-609).

Smith, R.S., and J. Klein, 1996, A special circumstance of airborne induced polarization measurements, *Geophysics*, 61, 66–73.

Viezzoli, Andrea & Fiandaca, Gianluca & Auken, Esben & Christiansen, Anders & Sergio, Simonetta. (2013). Constrained inversion of IP parameters from Airborne EM data. *ASEG Extended Abstracts*. 2013. 1. 10.1071/ASEG2013ab274.

Corresponding Author: francesco.dauti@unimi.it